Contents lists available at SciOpen

Food Science and Human Wellness

journal homepage: https://www.sciopen.com/journal/2097-0765

China Food Publishing Co.

Release profile and metabolism of bound polyphenols of oat bran during *in vitro* simulated gastrointestinal digestion and colonic fermentation

Yu Zhang[a,b,1], Bing Bai[a,1], Kai Huang[a,b], Sen Li[a,b], Hongwei Cao[a,b], Xiao Guan[a,b,*]

[a] *School of Health Science and Engineering, University of Shanghai for Science and Technology, Shanghai 200093, China*
[b] *National Grain Industry (Urban Grain and Oil Security) Technology Innovation Center, Shanghai 200093, China*

ARTICLE INFO

Article history:
Received 21 November 2023
Received in revised form 6 March 2024
Accepted 16 April 2024

Keywords:
Oat bran
Bound polyphenols
In vitro digestion
Colonic fermentation
Ferulic acid

ABSTRACT

Whole-grain foods have attracted emerging attention due to their health benefits. Whole grains are rich in bound polyphenols (BPs) linked with dietary fibers, which is largely underestimated compared with free polyphenols. In this study, *in vitro* simulated gastrointestinal digestion and colonic fermentation models were used to study the release profile and metabolism of BPs of oat bran. Significantly higher level of BPs was released during *in vitro* colon fermentation (3.05 mg GAE/g) than in gastrointestinal digestion (0.54 mg GAE/g). Five polyphenols were detected *via* LC-MS and their possible conversion pathways were speculated. Released BPs exhibited chemical antioxidant capacity. 16S rRNA sequencing further revealed that *Clostridium butyricum*, *Enterococcus faecalis*, *Bacteroides acidifaciens* were the key bacteria involved in the release of BPs, and this was verified by whole-cell transformation. Our results helped to explain the possible mechanism of the health benefits of BPs in whole grains.

© 2025 Beijing Academy of Food Sciences. Publishing services by Tsinghua University Press.
This is an open access article under the CC BY-NC-ND license
(http://creativecommons.org/licenses/by-nc-nd/4.0/).

1. Introduction

Polyphenols, as a major subcategory of phytochemicals, contribute to a key part in our daily diet. Many epidemiological studies have revealed the beneficial effects of polyphenols on health, such as antioxidant, anti-cancer and anti-diabetic activities[1-3]. However, most of the previous studies merely focus on free polyphenols, which can be directly extracted from organic solvents and are widely distributed in fruits and vegetables[4]. Still, a large part of bound polyphenols (BPs), which cannot be directly extracted from organic solvents and are bound to cell wall components, such as dietary fibers *via* chemically covalent bonds, hydrogen bonding and hydrophobic interactions, are ignored[5].

Whole-grain foods have been reported to exhibit benefits on health. Being different from fruits and vegetables, about 60%−85% of polyphenols in whole grains are BPs[6]. After solvent extraction, BPs can be extracted from the remaining solid residues through alkaline, acidic and enzymatic hydrolysis[7-8]. Also, studies by Zhang et al.[9] and Dong et al.[10] have revealed that gut microbiota were able to release BPs from dietary fibers of rice and carrot. They reported that the released BPs exhibit antioxidant activities and gut microbial composition was changed after *in vitro* fermentation with BPs bound with dietary fibers. Oat is rich in dietary fiber and polyphenols. Oat products are emerging as whole-grain foods with health benefits[11-13]. However, how BPs of oat behave during different stages of gastrointestinal and fermentation stages still lacks investigation. Key distinguished bacteria involves in the release and metabolism of BPs of oat have yet to be reported.

Thus, in the present study, we aimed to study the release profile and metabolism of BPs of oat bran *via in vitro* gastrointestinal and fermentation models. We prepared dietary fibers rich in BPs (DFBP) and insoluble dietary fiber (IDF) without BPs as a negative control. The composition and contents of BPs were analyzed by liquid

[1] Authors contributed equally to the work.
[*] Corresponding author at: School of Health Science and Engineering, University of Shanghai for Science and Technology, Shanghai 200093, China.
E-mail address: gnxo@163.com (X. Guan)
Peer review under responsibility of Beijing Academy of Food Sciences.

SciOpen Publishing services by Tsinghua University Press

http://doi.org/10.26599/FSHW.2024.9250239
2213-4530/© 2025 Beijing Academy of Food Sciences. Publishing services by Tsinghua University Press. This is an open access article under the CC BY-NC-ND license (http://creativecommons.org/licenses/by-nc-nd/4.0/).

chromatorgraph-mass spectrometer (LC-MS) during different stages of gastrointestinal and fermentation stages. Antioxidant activities of released BPs at different stages were compared by chemical antioxidant assays. Changes of gut microbiota were analyzed *via* 16S rRNA sequencing. Verification of gut bacteria involving in the release of BPs was performed using whole-cell transformation. Our results demonstrate the release and metabolism of BPs of oat to further explain the possible mechanism of the health benefits of BPs from whole-grains.

2. Materials and methods

2.1 Materials and reagents

Polyphenols standards were purchased from McLean (Shanghai, China), Sigma-Aldrich (Shanghai, China) and Aladdin Reagents (Shanghai, China). Methanol, and acetonitrile were purchased from Sinopharm Chemical Reagent Co., Ltd. (Shanghai, China). A total dietary fiber detection kit (K-TDFR 200 assays) was purchased from Megazyme (Wicklow, Ireland). Pepsin, α-amylase, and amyloglucosidase were purchased from Yuanye Biotechnology Co., Ltd. (Shanghai, China). *Clostridium butyricum* was purchased from Beijing Biobowell Biotechnology Co., Ltd. (Beijing, China). *Bacteroides acidifaciens* was purchased from Guangdong Microbial Culture Collection Center (Guangzhou, China). *Enterococcus faecalis* was purchased from Hebei Province Industrial Microbial Strains Engineering Technology Research Center (Hebei, China).

2.2 Preparation of DFBP and IDF

Preparation of DFBP was performed according to the previously described procedure with slight modification[9]. Oat bran was defatted and was ground to pass through an 80-mesh sieve. The defatted oat bran powder was mixed with water (1:10) and was gelatinized in a water bath (100 °C, 15 min), and then subjected to sequential enzymatic hydrolysis with 0.3% α-amylase (98 °C, 20 min), 0.5% protease (60 °C, 55 min), and 0.2% amyloglucosidase (60 °C, 30 min). After enzyme treatment, the mixture was centrifuged at 4 000 r/min for 10 min. The obtained precipitates were washed with 70%−80% ethanol and distilled water and then dried in a vacuum oven at 55 °C. The dried DFBP was stored at 4 °C until use.

IDF was prepared as previously reported[14-15]. Briefly, 1 g of DFBP was hydrolyzed with 20 mL of 2 mol/L NaOH at room temperature for 4 h with shaking. After hydrolyzation, the pH of the mixture was adjusted to 2.0 with 12 mol/L HCl. The mixture was centrifuged. The precipitate was washed to neutral and dried in an oven at 55 °C to obtain IDF. Contents of dietary fiber in DFBP and IDF determined by the total dietary fiber detection kit following the manufacturer's insctruction as previously reported[16].

2.3 In vitro digestion

In vitro digestion was performed as previously reported with slight modification[9]. Briefly, 1.5 g of DFBP was mixed with 20 mL of distilled water and adjusted to pH 2.0 with 6 mol/L HCl. Then 1 mL of gastric juice (5 g of pepsin dissolved in 250 mL of 0.1 mol/L HCl) was added to the mixture and was incubated in a shaking water bath (100 r/min) at 37 °C for 2 h to simulate gastric digestion. Afterwards, the pH of the digestive juice was adjusted to 7.2 with 1 mol/L $NaHCO_3$, and 7.5 mL of bile salt, pancreatin solution (1.2 g of bile salt and 0.2 g of pancreatin dissolved in 100 mL of 0.1 mol/L $NaHCO_3$) and 7.5 mL of NaCl/KCl mixture (7.02 g/L NaCl, 0.37 g/L KCl) were added to the mixture with shaking (100 r/min, 2 h) at 37 °C to simulate intestinal digestion. The reaction mixtures were centrifuged at 4 °C (10 000 r/min, 5 min) and the supernatants were stored at −80 °C until further analysis.

2.4 In vitro colonic fermentation

In vitro colonic fermentation was performed based on our previously published method[17-18]. Briefly, fresh feces were obtained from 5 donors (2 males and 3 females) aged between 20−26 years old (18 kg/m^2 < BMI < 25 kg/m^2) without bowel disease history and had not been treated with antibiotics for at least 3 months before fecal collection. Equal amounts of the fecal samples from each donor were homogenized under anaerobic conditions immediately after sample collection and then diluted to 10% (*m*/*V*) with sterile buffer to make the microbial solution. Freeze-dried residues of DFBP and IDF after gastrointestinal digestion were used for the following *in vitro* fermentation as the fermentation substrates. The groups were divided as follows: the Control group, positive control group (methyl ferulate, MF), DFBP group, and IDF group. A total of 20 mL of the microbial solution was mixed with 0.5 g of fermentation substrates. Samples were fermented in an anaerobic environment (90% of nitrogen, 5% of carbon oxide, and 5% of hydrogen) at 37 °C. At different time intervals (0.3, 6, 12, 24, and 48 h), 2 mL of the slurries was centrifuged and stored at −80 °C for further analysis. The pellet was further used for 16S rRNA, confocal laser scanning microscopy and Fourier transform infrared (FT-IR) analysis. The supernatant was further used for determination of BPs content, short-chain fatty acids (SCFAs), 2,2′-azino-bis (3-ethylbenzothiazoline-6-sulfonic acid) (ABTS) and 2,2-diphenyl-1-picrylhydrazyl (DPPH).

2.5 Determination of phenolic contents

Phenolic contents of samples were performed based on our previously reported method by the Folin-Ciocalteu method[8]. Absorbance was measured at 760 nm. The total phenolic content was expressed as milligrams of gallic acid equivalents (GAE) per 1 g of DFBP dry weight (DW).

2.6 Analysis of the composition of phenolic compounds

HPLC-UV-ESIMS analysis was performed on a Waters Acquity I-Class platform coupled with a Bruker Esquire 3000 Plus ion trap mass spectrometer (Bruker-Franzen Analytik GmbH, Bremen, Germany). The mobile phase consisted of mobile phase A (1% formic acid) and mobile phase B (95% methanol and 5% acetonitrile). A XTERRA RP C_{18} (250 × 4.6 mm, 5 μm) column was used for separation. The flow rate was 0.8 mL/min and the column temperature was maintained at 45 °C. The elution program was as follows: 0−45 min, 60% B; 45−47 min, 100% B; 47−50 min, 100% B; 50−60 min, 0% B. The injection volume was 20 μL and the UV detection wavelength was set at 280 nm. Commercial standards were used for the quantification of specific polyphenols. The standard

curve of peak area and concentration exhibited linearity within the range of 1−50 μg/mL ($R^2 > 0.999$). For the quantification of each phenolic compound, three independent experiments were conducted, and the results were expressed in μg/g DW.

2.7 Microstructural observation of samples

Confocal laser scanning microscopy (CLSM): microstructural changes of DFBP and IDP were observed with a confocal laser scanning microscope (LSM710 NLO, Zeiss, Gottingen, Germany) with 20× objective lenses. DFBP was dyed with a fluorescent dye solution containing 1 mg/mL Congo red. Images of dietary fiber were collected with 488 nm excitation, and images of phenolic substances were collected with 406 nm excitation.

Scanning electron microscopy (SEM): samples were uniformly dispersed and affixed onto conductive tape. Subsequently, a conductive film was applied, and the microstructure was examined using a scanning electron microscope (Hitachi Regulus 8230) at an operating voltage of 3.0 kV, with microscope magnifications of 10 000×.

2.8 FT-IR analysis

Totally, 1 mg of sample was mixed evenly with 200 mg KBr and pressed into a pellet. The FT-IR spectrum of samples with KBr pellet was measured *via* an FT-IR spectroscopy (Thermo Scientific Nicolet IS5) (wave number range 400−4 000 cm^{-1})[19].

2.9 Determination of chemical antioxidant activities

The DPPH and ABTS assays were performed based on previously reported method briefly[8,20]. 10 μL of sample solution was mixed with 200 μL of DPPH or ABTS working solution. Absorbance was measured at 517 nm for the DPPH assay and 734 nm for the ABTS assay using a BioTek Synergy HTX multi-mode reader (SYNERGY HTX, Japan). The free radical scavenging rate was calculated as: [1-(As-Ab)/Ac] × 100% (As: sample, Ab: equal volume of anhydrous methanol instead of DPPH/ABTS, Ac: equal volume of anhydrous methanol instead of sample).

2.10 16S rRNA gene sequencing

Microbial community genomic DNA was extracted using the TruSeqTM DNA sample prep kit (Omega Bio-tek, Georgia, U.S.) according to manufacturer's instructions. The concentration and purity were determined with a NanoDrop 2000 UV-Vis spectrophotometer (Thermo Scientific, Wilmington, USA). The hypervariable region V3–V4 of the bacterial 16S rRNA gene were amplified with primer pairs 338F (5′-ACTCCTACGGGAGGCAGCAG-3′) and 806R (5′-GGACTACHVGGGTWTCTAAT-3′) by an ABI GeneAmp® 9700 PCR thermocycler (ABI, CA, USA). The sequencing of 16S rRNA was conducted by Majorbio Bio-Pharm Technology Co., Ltd. Purified amplicons were pooled in equimolar and paired-end sequenced on an Illumina MiSeq PE300 platform/NovaSeq PE250 platform (Illumina, San Diego, USA) according to the standard protocols. The taxonomy of each operational taxonomic units (OTU) representative sequence was analyzed by RDP Classifier version 2.13 against the 16S rRNA database (eg. Silva v138) using the confidence threshold of 0.7. Analysis of the Shannon index, principal co-ordinates analysis (PCoA), LEfSe and Spearman coefficient were performed with online platform at https://cloud.majorbio.com/.

2.11 Whole-cell transformation

Whole-cell transformation was performed based on a previously reported method with slight modification[21]. *E. faecalis*, *B. acidifaciens*, and *C. butyricum* were inoculated into 50 mL medium with an inoculum volume of 1%. After culturing for 60 h, the mixture was centrifuged at 10 000 r/min for 10 min. The supernatant was discarded, and the pellet was washed twice with phosphate buffer (0.02 mol/L, pH 7.0). The pellet was resuspended in 5 mL of phosphate buffer solution with 2.5% MF. After incubating in a shaking water bath at 37 °C for 24 h, the resuspension was centrifuged and the content of whole-cell transformed ferulic acid in the supernatant was determined using HPLC-DAD as described above.

2.12 SCFAs analysis

Determination of SCFAs was done as previously reported with slight modification[16]. In brief, 0.9 mL of fermentation supernatant was mixed with 100 μL of hydrochloric acid. 2 mL of diethyl ether was then added and the extraction lasted for 20 min. The mixture was centrifuged at 3 000 r/min for 5 min to obtain the supernatant. Then, 500 μL of 1 mol/L NaOH was added. After 20 min, the mixture was centrifuged at 3 000 r/min for 5 min. The water phase was obtained and 100 μL of 12 mol/L HCl was added. The mixture was filtered through a microporous filter membrane (0.22 μm) for further analysis.

A LC-MS/MS ExionLC AD system was used for analysis of SCFAs. 20 μL of sample was injected onto a XTERRA RP C_{18} (250 × 4.6 mm, 5 μm) column at 30 °C. Mobile phase A was 0.025% phosphoric acid, and mobile phase B was acetonitrile. The flow rate was 1.0 mL/min. Isocratic elution was performed (mobile phase A:B = 95:5) for 15 min. The concentration of SCFAs in the sample was calculated based on the retention time and the integrated peaks of the standard curves for acetic acid, propionic acid, and butyric acid.

2.13 Statistical analysis

All data from were presented as the mean ± standard deviation (SD) and analyzed *via* GraphPad Prism version 9.0 (GraphPad Software, San Diego, USA). The means were compared using ordinary one-way analysis of variance (ANOVA) followed by Tukey's multiple comparison tests. Statistically significant differences were set at $P < 0.05$.

3. Results and discussion

3.1 BPs were released by gut microbiota and showed improved chemical antioxidant activities

How BPs behave under gastrointestinal and fermentation conditions was analyzed by *in vitro* simulated gastrointestinal digestion and fermentation models. The total content of BPs in DFBP was about (5.96 ± 0.13) mg GAE/g DW. As shown in Fig. 1A, after *in vitro* gastrointestinal digestion, only (0.54 ± 0.01) mg GAE/g DW

of BPs were released. This suggests that gastrointestinal conditions were too mild to break the ester bond that bind the primary link between BPs and dietary fiber[22]. Similar results were also observed in some previous studies[9-10,14]. Afterwards, an *in vitro* fermentation model was applied to evaluate whether gut microbiota could release or metabolize BPs. The content of released BPs from dietary fiber increased from (1.84 ± 0.01) mg GAE/g DW at 0.3 h to (3.05 ± 0.01) mg GAE/g DW at 24 h, indicating that BPs were gradually released from DFBP under the action of gut microbiota[14]. The content of released BPs decreased at 48 h, which was consistent with some previous studies, indicating that the released polyphenols might be metabolized by the gut microbiota[10].

Antioxidant activities of the released BPs of DFBP under different gastrointestinal digestion and fermentation stages were evaluated by ABTS and DPPH assays (Figs. 1B and C). Since a very little amount of BPs were released during gastrointestinal digestion, the free radical scavenging rates were pretty low (less than 10%). However, the free radical scavenging rate of supernatants increased significantly from 6 h (41.40%) to 24 h (62.80%) as the fermentation proceeded. This trend was in line with the significant elevation of released BPs during that period. After a 48-h fermentation, the free radical scavenging rates started to drop, which might be due to the degradation of released BPs into some small molecules with less antioxidant activity[14].

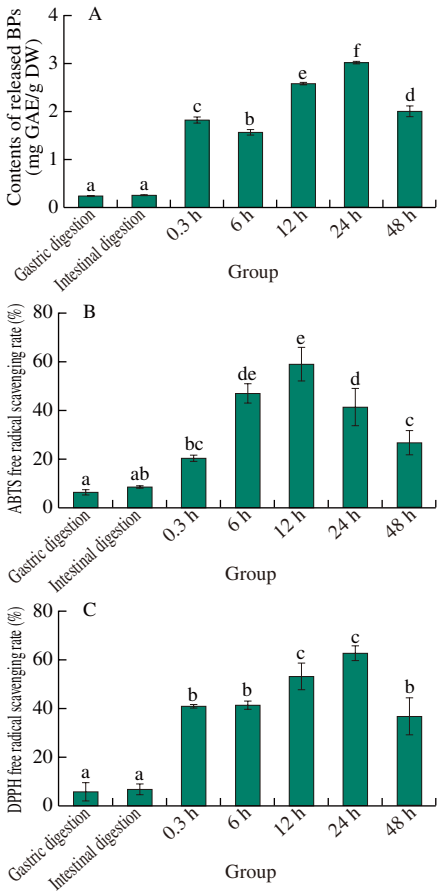

Fig. 1 Contents of released BPs and antioxidant activities during *in vitro* gastrointestinal digestion and fermentation. (A) Contents of released BPs from DFBP during each stage of *in vitro* gastrointestinal and fermentation stages. GAE: gallic acid equivalent. (B) ABTS and (C) DPPH activities of the released BPs during each stage of *in vitro* gastrointestinal and fermentation stages. Results are expressed as mean ± SD. Different letters refer to significant differences at $P < 0.05$.

3.2 Microstructural changes of DFBP after in vitro fermentation

SEM, CLSM and FT-IR were used to observe the microstructure of DFBP and IDF during fermentation (Fig. 2). SEM images revealed that both DFBP and IDF samples exhibited a smooth and uniform surface morphology without obvious convex or granular structures (Fig. 2A). After a 48-h fermentation, the DFBP images revealed a rough texture with evident concave-convex features, indicating significant structural changes induced by fermentation. In CLSM images, polyphenols were dyed in red and dietary fiber was dyed in green. Before *in vitro* fermentation, BPs bound with dietary fibers in DFBP can be observed, while red fluorescent signals cannot be observed in IDF (Fig. 2B). The red fluorescent signal in DFBP was attenuated after a 48-h *in vitro* fermentation and the gaps in the fiber structure became larger. This suggested that specific enzymes, such as esterase produced by gut microbiota broke down the bonds between fibers and fiber-linked polyphenols, and thus more BPs were released[23]. The fiber structure in IDF was looser after fermentation, suggesting that gut microbiota utilized IDF as nutrients[24].

Further, FT-IR images showed the cleavage of ester bonds connecting BPs and fibers in DFBP (Fig. 2C). The ester bond has 2 stretching vibration absorptions in the infrared spectrum. One has 2 C–O stretching vibration absorptions in the 1 300−1 050 cm^{-1} region, where DFBP has 2 peaks, indicating the presence of ester bonds, while IDF does not have. The other is around 1 735 cm^{-1} that C=O absorbs more than C=C–COOR or ArCOOR, and moves closer to C=C conjugation to low wavenumber[1]. Both DFBP and IDF did not change significantly before and after fermentation around 1 735 cm^{-1}. Taken these results together, gut microbiota could utilize dietary fiber in DFBP and break the ester bonds within it, thereby releasing BPs.

3.3 Microbial composition after in vitro fermentation

16S rRNA gene sequencing was performed to further analyze the composition of microbial composition after *in vitro* fermentation with DFBP, IDF and methyl ferulate (MF, used as a positive control). At phylum level (Fig. 3A), Firmicutes contributed to the major part of gut microbiota for over 60% in all groups. Compared with the Control group, fermentation with IDF increased the abundance of Firmicutes, while significantly reduced the abundance of *Fusobacteriota*. Fermentation with DFBP remained the abundance of Firmicutes unchanged, while significantly increased the abundance of *Proteobacteria* and reduced the abundance of *Bacteroidota* (Figs. 3B and C). PCoA and PLS-DA analysis revealed that the clusters of the Control, MF, DFBP, and IDF groups separated obviously, indicating the different composition of gut microbiota in different groups (Figs. 3D and S1A). Comparison between Control *vs*. DFBP, DFBP *vs*. IDF and DFBP *vs*. MF were shown in Figs. 3E, F, and S1C, respectively. Distinguished bacteria in each group at genus level were revealed by Cladogram (Fig. 3G) and LefSe analysis (Fig. S1B). Results showed that *Clostridium sensu stricto* 1 and *Enterococcus* were the distinguished bacteria in the DFBP group. These 2 bacteria were the common bacteria that were enriched in both DFBP and IDF groups, indicating that they were able to utilize fiber in IDF and DFBP. Previous studies also reported similar results[24]. For *Clostridium sensu stricto* 1, it appeared as a distinguished

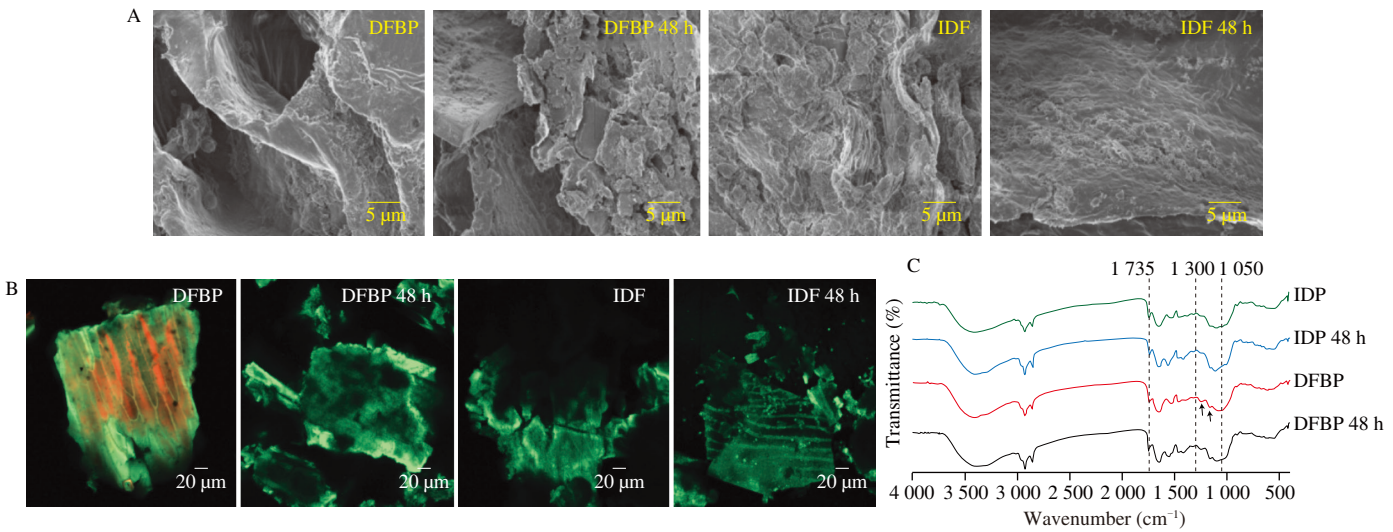

Fig. 2 Structural changes of DFBP and IDF before and after *in vitro* fermentation. (A) SEM images and (B) CLSM images of DFBP, IDF before/after a 48-h fermentation. (C) FT-IR spectra of DFBP and IDF before and after a 48-h *in vitro* fermentation.

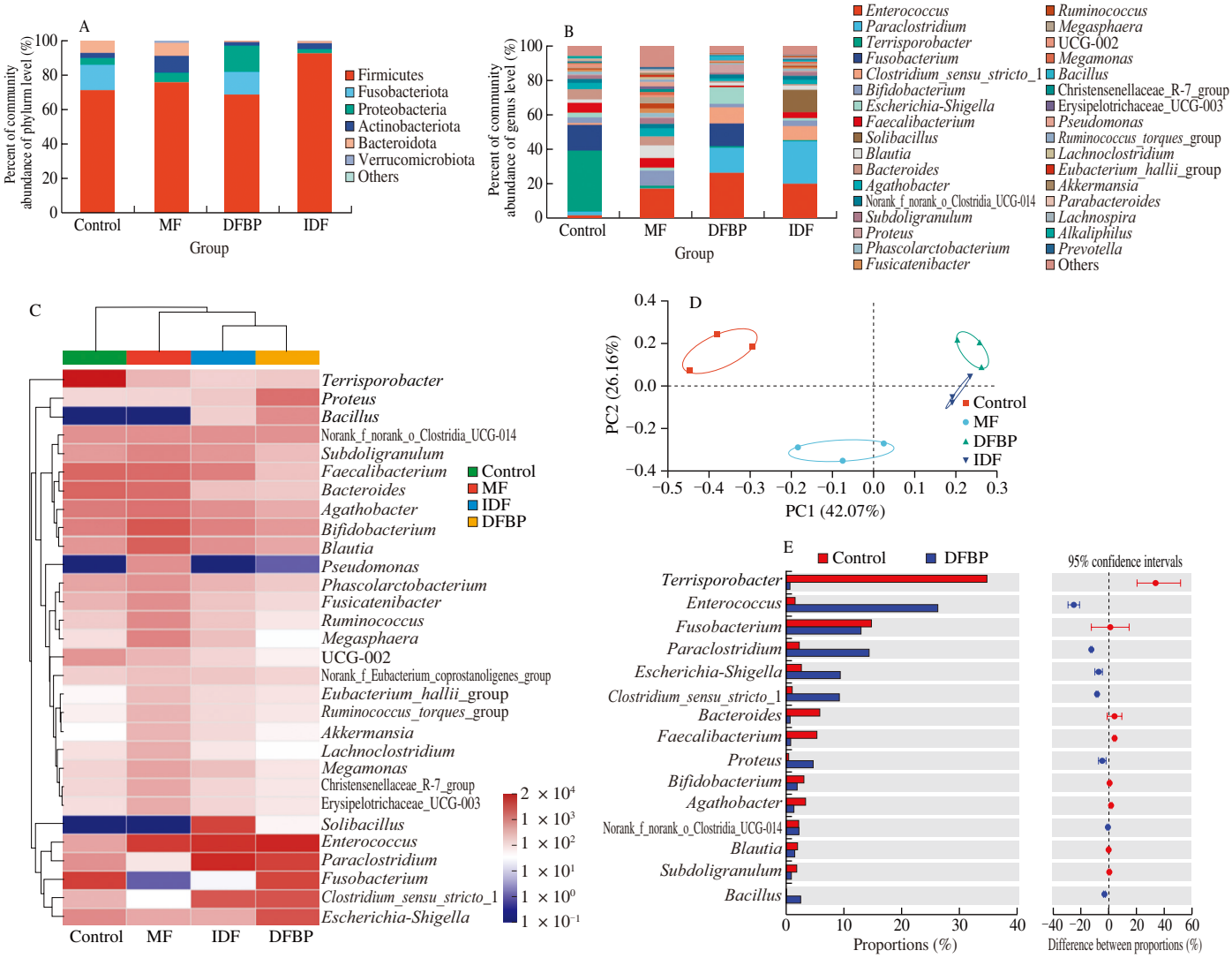

Fig. 3 Composition of gut microbiota of the Control, MF, DFBP, and IDF groups after a 24-h *in vitro* fermentation. Composition of gut microbiota of the Control, MF, DFBP, and IDF groups at (A) phylum level and (B) genus level. (C) A heat map of the bacteria at genus level. (D) PCoA analysis of gut microbiota among the Control, MF, DFBP, and IDF groups. Two groups comparison of Wilcoxon rank-sum test bar plot at genus level among (E) Control *vs*. DFBP groups and (F) DFBP *vs*. IDF groups. (G) Cladogram showing the phylogenetic distribution of the gut microbiota community from 4 different groups from LEfSe analysis of the key genera of gut microbiota (linear discriminant analysis (LDA) = 3).

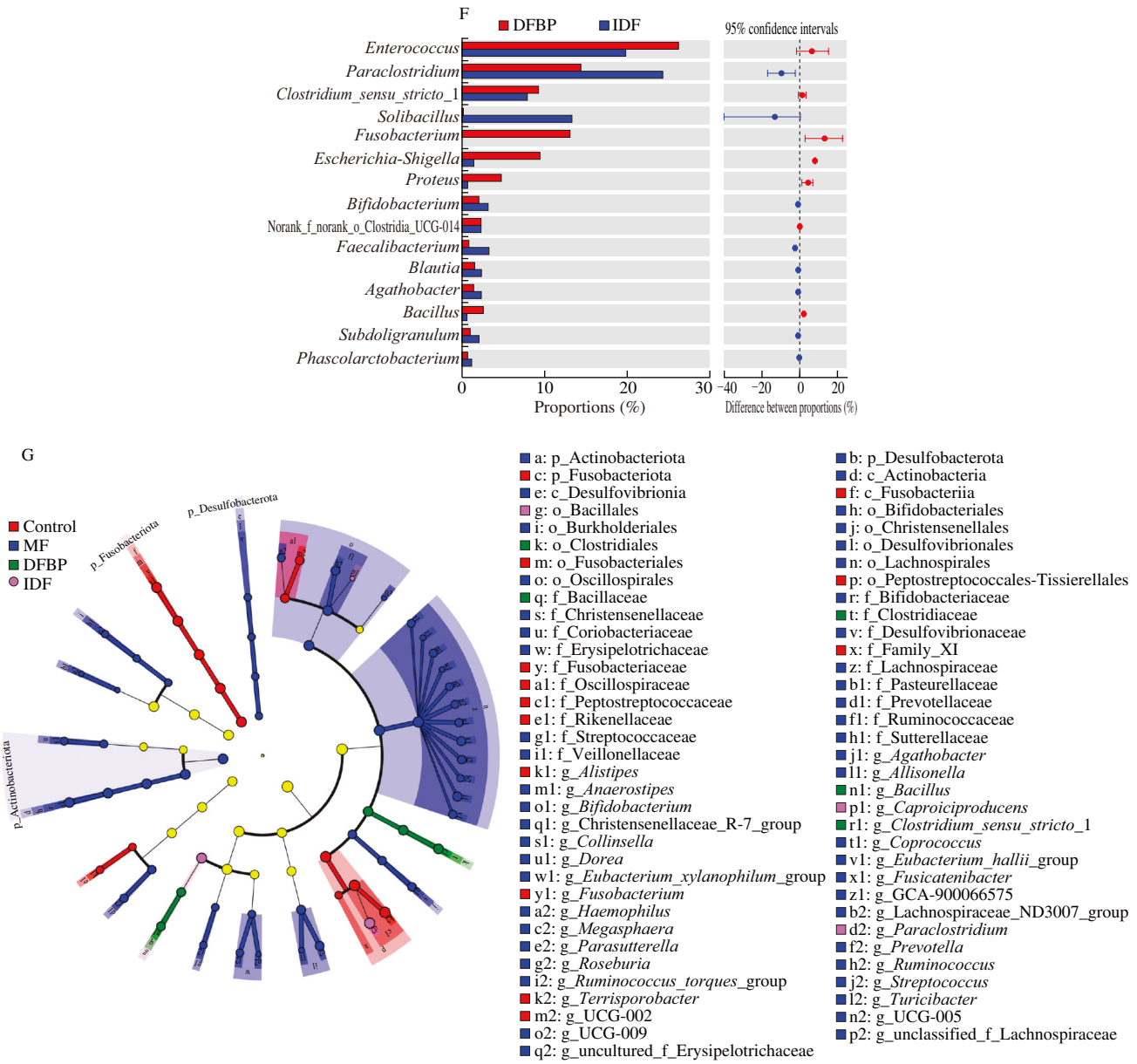

Fig. 3 (*Continued*)

bacterium in the DFBP group when compared with either the IDF or MF group. This indicates that it might involve in the release or metabolism of BPs in DFBP, since DFBP contained BPs, while IDF did not. For *Enterococcus*, it was reported to release ferulic acid after solid fermentation of wheat bran in a previous study[25]. This was in line with our findings.

3.4 Production of SCFAs and composition of the released BPs of DFBP during in vitro fermentation

Since DFBP and IDF both contained dietary fiber, it could be utilized by gut microbiota and produced SCFAs. Contents of SCFAs were further quantified to evaluate the utilization of dietary fiber by gut microbiota after fermentation with DFBP. Production of acetic acid, propionic acid and butyric acid showed upward trends (Figs. 4B-D), which can also be reflected in the decreasing value of pH as the fermentation processed (Fig. 4A). After a 24-h fermentation, acetic acid and butyric acid contributed to the major composition of total SCFAs, and they could be used as the energy source for gut microbiota[26-27]. SCFAs production in the IDF group was generally higher than that in the DFBP group, including acetic acid and butyric acid. Structurally, the major difference between DFBP and IDF was the existence of BPs in DFBP. Although dietary fiber in DFBP contributed to some amount of SCFAs production, the produced phenolic acids from the interaction between BPs and gut microbiota might to some extent inhibit the growth of bacteria, which played a key role in SCFAs production in gut[28-29]. This might explain a lower production of SCFAs in the DFBP group, compared with the IDF group. Proportion of SCFAs depends on the composition of gut microbiota and content of dietary fiber[30]. 16S rRNA sequencing showed that *Enterococcus* and *Clostridium* were the common bacteria that were enriched after fermentation of both DFBP and IDF (Figs. 3E and F). These bacteria were reported to be involved in the production of SCFAs[31-33], which was in consistency with our findings.

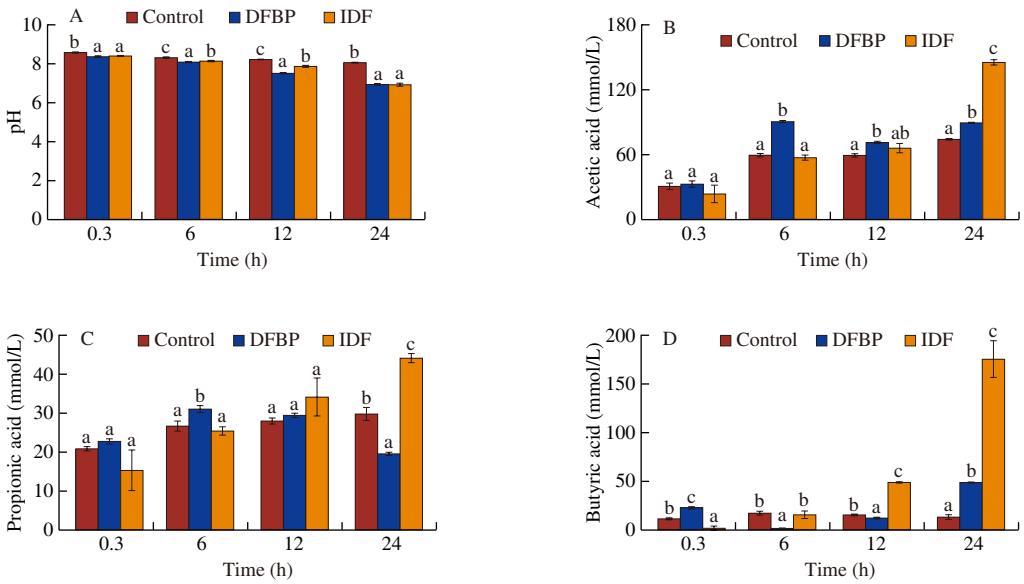

Fig. 4 Changes of pH and production of SCFAs of DFBP at different stages of *in vitro* fermentation. (A) Changes of pH of the Control, DFBP, and IDF groups at different stages of *in vitro* fermentation. Contents of (B) acetic acid, (C) propionic acid and (D) butyric acid in different groups at different stages of fermentation. Different lowercase letters represent significant differences in the same substance content at the same time ($P < 0.05$).

To further confirm the composition of released BPs during each stage of *in vitro* colonic fermentation, LC-MS analysis was performed. Vanillic acid, *p*-coumaric acid, *p*-hydroxybenzoic acid, ferulic acid and syringic acid were detected and shown to be the major released BPs in the HPLC chromatogram (Fig. S2). Contents of these phenolic acids were quantified (Table 1). At the end of fermentation (24 h), contents of *p*-coumaric acid, vanillic acid and *p*-hydroxybenzoic acid decreased significantly, compared with those at 0.3 h. However, the content of ferulic acid increased significantly, from (31.37 ± 7.28) μg/g at 0.3 h to (156.53 ± 12.01) μg/g at 24 h. Ferulic acid is a representative phenolic acid existing in whole grains[15]. An increased content of ferulic acid after fermentation suggested that gut microbiota utilized DFBP and hydrolyzed dietary fiber to release bound ferulic acid. After ferulic acid was released, gut microbiota can further metabolize it to form other type of phenolic acids[32].

Table 1
Quantification of released bound polyphenols by HPLC-UV-ESIMS.

Compounds	0.3 h	6 h	12 h	24 h
Ferulic acid	31.37 ± 7.28^{a}	57.17 ± 13.45^{a}	39.64 ± 12.83^{ab}	156.53 ± 12.01^{c}
p-Coumaric acid	36.19 ± 7.26^{a}	26.21 ± 9.07^{ab}	33.37 ± 6.66^{a}	6.04 ± 4.27^{c}
Vanillic acid	30.24 ± 15.10^{ac}	15.85 ± 1.49^{ab}	47.00 ± 5.54^{c}	6.64 ± 4.29^{b}
Syringic acid	20.11 ± 5.01^{ab}	11.50 ± 1.59^{c}	15.67 ± 3.12^{bc}	23.80 ± 1.54^{a}
p-Hydroxybenzoic acid	25.32 ± 8.24^{ab}	12.36 ± 1.38^{c}	26.48 ± 2.18^{a}	14.66 ± 0.64^{bc}

Note: Results are expressed as mean ± SD, and different letters are significantly different in the same row ($P < 0.05$).

3.5 Possible conversion pathways of phenolic acids and involvement of gut microbiota

Gut microbiota utilized DFBP and IDF, and this process also promoted the release of BPs. Then, liberation of the above phenolic acids (Table 1) was probably due to the esterase produced by gut microbiota, which broke the ester bond between phenolic acids and dietary fiber[34]. Other than the esterase, other enzymes secreted by gut microbiota might also involve in the metabolism of the released BPs from DFBP, since the contents of released BPs changed at different fermentation stages[24]. Enzymes secreted by gut microbiota participating in the metabolism of polyphenols largely decide the production of metabolized polyphenols after fermentation. *Enterococcus* and *Clostridium* were enriched in the DFBP and IDF groups, and they have been reported to secrete ferulic acid esterase that involved in the process of dehydroxylation, *α*-oxidation, dehydrogenation, etc. For instance, Mao et al.[25] showed that after solid fermentation of wheat bran with *E. faecalis* M2, the content of total phenolic increased significantly, especially ferulic acid, which increased 5.5 times. *C. butyricum* is able to utilize dietary fiber as an energy source, and is capable of producing sialate *O*-acetylesterase and esterase, which also play a key role in releasing BPs bound with dietary fiber[35]. Thus, the content of ferulic acid increased the most (4 times more) after a 24-h fermentation. This was in line with these previous studies.

The possible metabolic pathways for the analyzed phenolic acids were proposed (Fig. 5). Gallic acid can be converted to syringic acid *via* methylation, and syringic acid can be converted to vanillic acid after demethoxylation[36]. Vanillic acid can be converted to protocatechuic acid and *p*-hydroxybenzoic acid *via* demethylation and dehydroxylation stepwise. Ferulic acid can be further converted to caffeic acid by demethylation, and then caffeic acid can be converted to coumaric acid by dehydroxylation[9]. After a 24-h fermentation, only ferulic acid increased the most, while *p*-coumaric acid, vanillic acid and *p*-hydroxybenzoic acid decreased significantly. This indicated that the process of releasing ferulic acid was mounting rapidly, and the gut-metabolized phenolic acids from ferulic acid might be further degraded to other smaller metabolites, such as catechol and benzoic acid with lower contents.

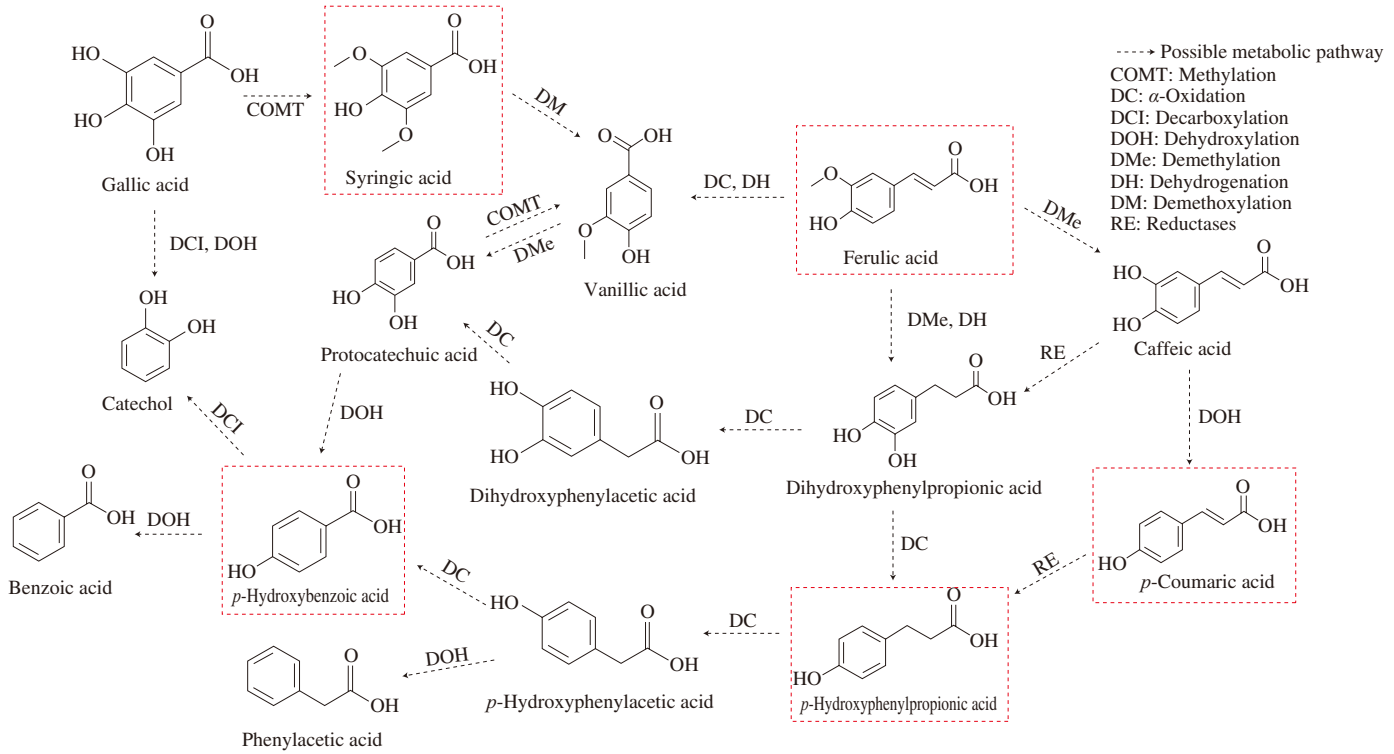

Fig. 5 Proposed metabolic pathways of BPs released from DFBP during *in vitro* colonic fermentation.

3.6 Verification of gut bacteria involved in the release of ferulic acid from DFBP

To further verify whether the key bacteria in the DFBP group could secret enzymes, such as esterase that can break the ester bond between BPs and dietary fiber, whole cell transformation was performed. By culturing *E. faecalis*, *C. butyricum* and *B. acidifaciens* with MF as the substrate, respectively, the production of ferulic acid was detected *via* HPLC (Fig. S3). Totally 5 mL of *E. faecalis* (3.1×10^9 CFU/mL), *B. acidifaciens* (2.8×10^9 CFU/mL) and of *C. butyricum* (1.6×10^9 CFU/mL) were cultured with MF for 24 h. The contents of produced ferulic acid were (1 050.98 ± 3.54), (695.92 ± 4.49) and (831.62 ± 1.77) μg/g after whole-cell transformation of *E. faecalis*, *B. acidifaciens* and *C. butyricum*, respectively. Compared with the other two bacteria, *C. butyricum* produced the most amount of ferulic acid, indicating its ability to release BPs from dietary fiber. Under the action of cellulase and esterase produced by some specific gut microbiota, cell wall would be destroyed, and thus ferulic acid and other BPs can be released.

4. Conclusion

Release profile and metabolism of BPs of oat bran were investigated *via in vitro* gastrointestinal and fermentation model. Gastrointestinal conditions were difficult to release BPs from DFBP, whereas gut microbiota during *in vitro* fermentation were able to release significantly higher level of BPs. Ferulic acid, *p*-coumaric acid, vanillic acid, syringic acid and *p*-hydroxybenzoic acid were the major released BPs from DFBP. Released BPs showed strong free radical scavenging activities. 16S rRNA sequencing revealed that *C. butyricum*, *E. faecalis*, *B. acidifaciens* were distinguished bacteria involved in the release of BPs, which was confirmed by whole-cell transformation assay. The process of releasing and metabolizing BPs of whole grains might contribute to the health mechanism of cereal polyphenols. Results of the present study were based on *in vitro* models. A deeper investigation of BPs-induced distinguished bacteria can be performed *in vivo* for the future development of synbiotics to improve gut oxidative stress.

Conflict of interest

The authors declare no competing financial interest.

Acknowledgments

We thank for the support from the research grants by National Natural Science Foundation of China (32202051), National Key R&D Program of China (2022YFF1100104) and the Major Project of Inner Mongolia Science and Technology Department, China (2021ZD0002).

References

[1] S. Liu, M. Jia, J. Chen, et al., Removal of bound polyphenols and its effect on antioxidant and prebiotics properties of carrot dietary fiber, Food Hydrocoll. 93 (2019) 284-292. http://doi.org/10.1016/j.foodhyd.2019.02.047.

[2] M.L. Contente, F. Annunziata, P. Cannazza, et al., Biocatalytic approaches for an efficient and sustainable preparation of polyphenols and their derivatives, J. Agric. Food Chem. 69 (2021) 13669-13681. http://doi.org/10.1021/acs.jafc.1c05088.

[3] S. Li, T. Liang, Y. Zhang, et al., Vitexin alleviates high-fat diet induced brain oxidative stress and inflammation *via* anti-oxidant, anti-inflammatory and gut microbiota modulating properties, Free Radical Biol. Med. 171 (2021) 332-344. http://doi.org/10.1016/j.freeradbiomed.2021.05.028.

[4] S.M. Aravind, S. Wichienchot, R. Tsao, et al., Role of dietary polyphenols on gut microbiota, their metabolites and health benefits, Food Res. Int. 142 (2021) 110189. https://doi.org/10.1016/j.foodres.2021.110189.

[5] Z. Wang, S. Li, S. Ge, et al., Review of distribution, extraction methods, and health benefits of bound phenolics in food plants, J. Agric. Food Chem. 68 (2020) 3330-3343. http://doi.org/10.1021/acs.jafc.9b06574.

[6] J. Li, H. Zhang, X. Yang, et al., Trapping of reactive carbonyl species by fiber-bound polyphenols from whole grains under simulated physiological conditions, Food Res. Int. 156 (2022) 111142. http://doi.org/https://doi.org/10.1016/j.foodres.2022.111142.

[7] Y. Zhang, Y. Yan, W. Li, et al., Microwaving released more polyphenols from black quinoa grains with hypoglycemic effects compared with traditional cooking methods, J. Sci. Food Agric. 102 (2022) 5948-5956. http://doi.org/10.1002/jsfa.11947.

[8] Y. Zhang, B. Bai, Y. Yan, et al., Bound polyphenols from red quinoa prevailed over free polyphenols in reducing postprandial blood glucose rises by inhibiting alpha-glucosidase activity and starch digestion, Nutrients 14 (2022) 728. http://doi.org/10.3390/nu14040728.

[9] X. Zhang, M. Zhang, L. Dong, et al., Phytochemical profile, bioactivity, and prebiotic potential of bound phenolics released from rice bran dietary fiber during *in vitro* gastrointestinal digestion and colonic fermentation, J. Agric. Food Chem. 67 (2019) 12796-12805. http://doi.org/10.1021/acs.jafc.9b06477.

[10] R. Dong, Q. Yu, W. Liao, et al., Composition of bound polyphenols from carrot dietary fiber and its *in vivo* and *in vitro* antioxidant activity, Food Chem. 339 (2021) 127879. https://doi.org/10.1016/j.foodchem.2020.127879.

[11] X. Li, L. Zhou, Y. Yu, et al., The potential functions and mechanisms of oat on cancer prevention: A review, J. Agric. Food Chem. 70 (2022) 14588-14599. http://doi.org/10.1021/acs.jafc.2c06518.

[12] L. Călinoiu, D. Vodnar, Thermal processing for the release of phenolic compounds from wheat and oat bran, Biomolecules 10 (2019) 21. http://doi.org/10.3390/biom10010021.

[13] Y. Yu, L. Zhou, X. Li, et al., The progress of nomenclature, structure, metabolism, and bioactivities of oat novel phytochemical: avenanthramides, J. Agric. Food Chem. 70 (2022) 446-457. https://doi.org/10.1021/acs.jafc.1c05704.

[14] J. Su, X. Fu, Q. Huang, et al., Phytochemical profile, bioactivity and prebiotic potential of bound polyphenols released from *Rosa roxburghii* fruit pomace dietary fiber during *in vitro* digestion and fermentation, Food Funct. 13 (2022) 8880-8891. https://doi.org/10.1039/D2FO00823H.

[15] Z. Feng, L. Dong, R. Zhang, et al., Structural elucidation, distribution and antioxidant activity of bound phenolics from whole grain brown rice, Food Chem. 358 (2021) 129872. https://doi.org/10.1016/j.foodchem.2021.129872.

[16] Y. Zhang, F. Li, B. Bai, et al., Milling degree affects the fermentation properties of rice: perspectives from the composition of nutrients and gut microbiota *via in vitro* fermentation, Food Sci. Hum. Wellness 13 (2024) 1578-1588. https://doi.org/10.26599/FSHW.2022.9250133.

[17] S. Li, L. Luo, S. Wang, et al., Regulation of gut microbiota and alleviation of DSS-induced colitis by vitexin, Eur. J. Nutr. 62 (2023) 3433-3445. https://doi.org/10.1007/s00394-023-03237-2.

[18] J. Chen, Y. Zhang, X. Guan, et al., Characterization of saponins from differently colored quinoa cultivars and their *in vitro* gastrointestinal digestion and fermentation properties, J. Agric. Food Chem. 70 (2022) 1810-1818. http://doi.org/10.1021/acs.jafc.1c06200.

[19] P. Lixourgioti, K.A. Goggin, X. Zhao, et al., Authentication of cinnamon spice samples using FT-IR spectroscopy and chemometric classification, LWT-Food Sci. Technol. 154 (2022) 112760 http://doi.org/10.1016/j.lwt.2021.112760.

[20] D. Liang, B. Feng, N. Li, et al., Preparation, characterization, and biological activity of *Cinnamomum cassia* essential oil nano-emulsion, Ultrason. Sonochem. 86 (2022) 106009. http://doi.org/10.1016/j.ultsonch.2022.106009.

[21] X. Wang, R. Su, K. Chen, et al., Engineering a microbial consortium based whole-cell system for efficient production of glutarate from *L*-lysine, Front. Microbiol. 10 (2019) 341. https://doi.org/10.3389/fmicb.2019.00341.

[22] Z.H. Xu, X. Xiong, Q.Z. Zeng, et al., Alterations in structural and functional properties of insoluble dietary fibers-bound phenolic complexes derived from lychee pulp by alkaline hydrolysis treatment, LWT-Food Sci. Technol. 127 (2020) 109335. https://doi.org/10.1016/j.lwt.2020.109335.

[23] G. Rocchetti, R.P. Gregorio, J.M. Lorenzo, et al., Functional implications of bound phenolic compounds and phenolics–food interaction: a review, Compr. Rev. Food Sci. Food Saf. 21 (2022) 811-842. http://doi.org/10.1111/1541-4337.12921.

[24] M. Makarewicz, I. Drozdz, T. Tarko, et al., The interactions between polyphenols and microorganisms, especially gut microbiota, Antioxidants 10 (2021) 188. http://doi.org/10.3390/antiox10020188.

[25] M. Mao, P. Wang, K. Shi, et al., Effect of solid state fermentation by *Enterococcus faecalis* M2 on antioxidant and nutritional properties of wheat bran, J. Cereal Sci. 94 (2020) 102997. http://doi.org/10.1016/j.jcs.2020.102997.

[26] A. Nogal, A.M. Valdes, C. Menni, The role of short-chain fatty acids in the interplay between gut microbiota and diet in cardio-metabolic health, Gut Microbes 13 (2021) 1-24. http://doi.org/10.1080/19490976.2021.1897212.

[27] J.K. Tan, L. Macia, C.R. Mackay, Dietary fiber and SCFAs in the regulation of mucosal immunity, J. Allergy Clin. Immunol. 151 (2023) 361-370. http://doi.org/10.1016/j.jaci.2022.11.007.

[28] I. Antonopoulou, E. Sapountzaki, U. Rova, et al., Ferulic acid from plant biomass: a phytochemical with promising antiviral properties, Front. Nutr. 8 (2022) 777576. https://doi.org/10.3389/fnut.2021.777576.

[29] A. Koh , F.D. Vadder , P.K. Datchary, et al., From dietary fiber to host physiology: short-chain fatty acids as key bacterial metabolites, Cell 165 (2016) 1332-1345. https://doi.org/10.1016/j.cell.2016.05.041.

[30] L.Y. Hou, Y.E. Yang, B.S. Sun, et al., Dietary fiber, gut microbiota, short-chain fatty acids, and host metabolism, Am. J. Life Sci. 9 (2021) 162-172. https://doi.org/10.11648/j.ajls.20210906.12.

[31] W. Xu, K. Zou, Y. Zhan, et al., *Enterococcus faecium* GEFA01 alleviates hypercholesterolemia by promoting reverse cholesterol transportation *via* modulating the gut microbiota-SCFA axis, Front. Nutr. 9 (2022) 1020734. https://doi.org/10.3389/fnut.2022.1020734.

[32] B. Zhang, Y. Zhang, H. Li, et al., A review on insoluble-bound phenolics in plant-based food matrix and their contribution to human health with future perspectives, Trends Food Sci. Tech. 105 (2020) 347-362. http://doi.org/10.1016/j.tifs.2020.09.029.

[33] Y.S. Jang, H.M. Woo, J.A. Im, et al., Metabolic engineering of *Clostridium acetobutylicum* for enhanced production of butyric acid, Appl. Microbiol. Biot. 97 (2013) 9355-9363. https://doi.org/10.1007/s00253-013-5161-x.

[34] C. Kmezik, S. Mazurkewich, T. Meents, et al., A polysaccharide utilization locus from the gut bacterium dysgonomonas mossii encodes functionally distinct carbohydrate esterases, J. Biol. Chem. 296 (2021) 100500. https://doi.org/10.1016/j.jbc.2021.100500.

[35] M.S. Kannisto, R.K. Mangayil, A. Shrivastava-Bhattacharya, et al., Metabolic engineering of acinetobacter baylyi ADP1 for removal of *Clostridium butyricum* growth inhibitors produced from lignocellulosic hydrolysates, Biotechnol. Biofuels 8 (2015) 1-10. https://doi.org/10.1186/s13068-015-0389-6.

[36] E. Turrini, F. Maffei, A. Milelli, et al., Overview of the anticancer profile of avenanthramides from oat, Int. J. Mol. Sci. 20 (2019) 4536. https://doi.org/10.3390/ijms20184536.